

FEM analysis of expandable intramedullary nails in healthy and osteoporotic femur

W. Kajzer*, A. Kajzer, J. Marciniak

Division of Biomedical Engineering, Institute of Engineering Materials and Biomaterials, Silesian University of Technology,
ul. Konarskiego 18a, 44-100 Gliwice, Poland

* Corresponding author: E-mail address: wojciech.kajzer@polsl.pl

Received 25.09.2009; published in revised form 01.12.2009

Analysis and modelling

ABSTRACT

Purpose: The paper presents the results of numerical analysis of expandable intramedullary nail – femur system in different states of healing. The aim of the research was to determine displacements, deformations and stresses occurring in a bone depending on the age of the patient and the extent level of osteoporosis.

Design/methodology/approach: A femur was selected to numerical analysis. The analysis concerned the influence of the load and torsion of the system on the obtained results of displacements, deformations and reduced stresses. In order to make calculations, four models with different mechanical properties were chosen: model 1: femur with mechanical properties corresponding with a femur of a patient at the age of 16, model 2: with mechanical properties corresponding with a femur of a patient at the age of about 28, model 3: with mechanical properties corresponding with a femur of a patient at the age of about 20 and at the age of 50 to 65 years old and model 4: with mechanical properties corresponding with a femur of a patient at the age above 70 or with osteoporosis. For the chosen model of intramedullary nail, mechanical properties of titan alloy Ti-6Al-4V were used. Two load steps were analyzed: load step 1 in which simple axial load with a value ranging from 250 up to 1000 N simulating patient standing on one leg was used, and load step 2 – a torsion analyzing loads that the nail is exposed to while walking.

Findings: Conducted analysis of the system showed the difference in displacements, deformations and reduced stresses depending on assumed mechanical properties of femur and load step of the system.

Research limitations/implications: The limitations were connected with the necessity of simplifying the assumptions, which were associated with limitations caused by boundary conditions. In researches 4 forces loading the femur axially were used: 1: force $F = 250\text{N}$, 2: with force $F = 500\text{N}$, 3: with force $F = 750\text{N}$ and 4: with force $F = 1000\text{N}$ and 5 values of angle displacement of the femur head were assumed: 1: angle displacement $\varphi = 1^\circ$, 2: $\varphi = 5^\circ$, 3: $\varphi = 10^\circ$, 4: $\varphi = 15^\circ$, 5: $\varphi = 20^\circ$.

Practical implications: Obtained results can be applied in selection of stabilization methods of bone fragments and in forecasting biomechanical conditions depending on the age of patient and the state of his general conditions of bones.

Originality/value: The paper presents the displacement-deformation-stress characteristics of femur - expandable intramedullary nail system, using the Finite Elements Method (FEM) in the analysis.

Keywords: Numerical analysis; Biomechanical analysis; Biomaterials; Mechanical properties of bones

Reference to this paper should be given in the following way:

W. Kajzer, A. Kajzer, J. Marciniak, FEM analysis of expandable intramedullary nails in healthy and osteoporotic femur, Journal of Achievements in Materials and Manufacturing Engineering 37/2 (2009) 563-570.

1. Introduction

From the biomechanical point of view, determination of hard tissues structure is crucial. Knowledge of the properties is essential, both in diagnosis of bone system illnesses as well as in selection of implants' mechanical properties. Stiffness of a bone – implant system is particularly important.

Young modulus of bone changes with age Fig. 1. It is related with demineralization of bone. Increase of bone porosity is caused by different factors, for example osteoporosis which is characterized by decrease of bone mass, disordered microarchitecture of bone and, as a consequence, decreased mechanical strength. These factors lead to increase of fracture risk.

Literature data indicate that maximum mass of bone tissue is reached in adults (approximately 30 years old). In this age, metabolism of bone is stabilized and osteoblastic and osteoclastic processes are in equilibrium. After the age of 40 intensification of osteoblastic effects is reduced and demineralization processes start to dominate that causes loss of bone mass. In this way, about 0.5-1.0% of minerals per year are lost. However, in osteoporotic bone the loss is in the range 2-5 % per year. That is why the osteoporotic bone is porous and brittle [1].

Knowledge of material data and mechanical properties of bone tissue (tensile, bending and torsional strength) allows to evaluate stresses and strains in bones and select mechanical properties of implants [1, 2, 4-18].

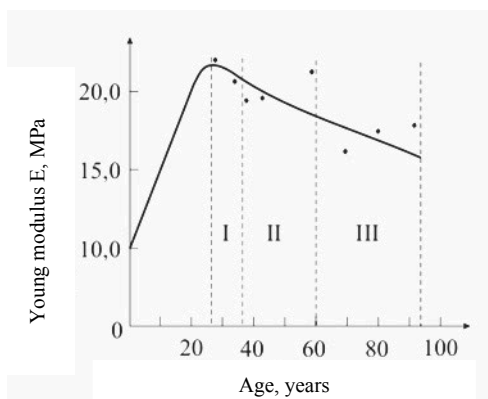


Fig. 1. Dependence between Young modulus and human age [1,3]

2. Material and methods

Numerical model of femur, worked out in Laboratorio di Tecnologia dei Materiali, Istituti Ortopedici Rizzoli, was applied in the biomechanical analysis of the expandable intramedullary nail. In order to conduct the analysis, following mechanical properties of femur based on Fig.1 were taken into consideration: model 1:femur with mechanical properties corresponding with a femur of a patient at the age of 16, Young's module $E = 16000$ MPa, Poisson's ratio $\nu = 0.44$, model 2- with mechanical properties corresponding with a femur of a patient at

the age of about 28 - $E = 22000$ MPa $\nu = 0.44$, model 3- with mechanical properties corresponding with a femur of a patient at the age of about 20 and at the age of 50 to 65 years old - $E = 18600$ MPa, $\nu = 0.44$ and model 4 - with mechanical properties corresponding with a femur of a patient at the age above 70 or with osteoporosis - $E = 17400$ MPa, $\nu = 0.44$.

Geometrical model of expandable intramedullary nail was prepared in ANSYS. The following mechanical properties were selected: Ti-6Al-4V alloy: $E = 1.1 \cdot 10^5$ MPa, Poisson's ratio $\nu = 0.33$.

Geometrical model of the analyzed femur - expandable intramedullary nail system was presented in Fig. 2. The analysis was carried out for proximal simple fracture (100 mm below trochanter) – Fig. 3. Fracture gap was equal to 0.1 mm.

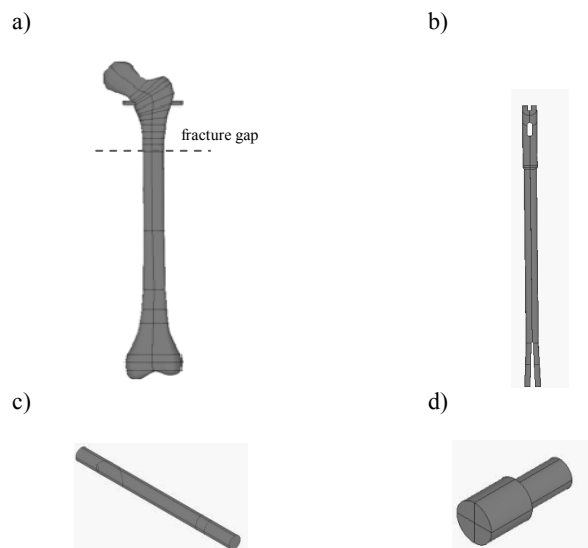


Fig. 2. Geometrical model of the femur - expandable intramedullary nail system: a) view of the system, b) expandable intramedullary nail, c) lock, d) blocking screw

On the basis of the geometrical models a finite element mesh was generated – Fig 3a. The meshing was realized with the use of the SOLID95 element – Fig. 3b. This type of element is used for the three-dimensional modeling of solid structures. The element is defined by eight nodes having three degrees of freedom at each node: translations in the nodal x, y, and z directions.

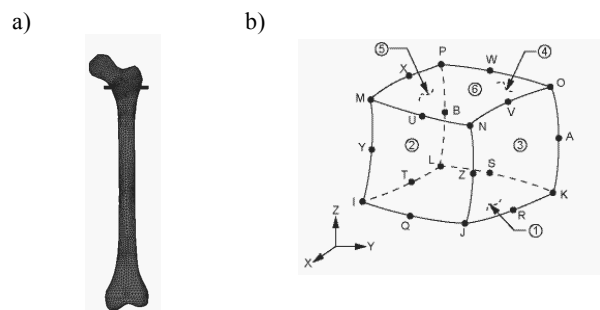


Fig. 3. a) Discrete model of the femur -expandable intramedullary nail system, b) The SOLID 95 finite element

- The calculations were carried out for two load steps - Fig. 4:
- compressing with the force of 250, 500, 750, 1000N,
 - torsion with the assumed radial displacement of the femur head with the torsional angle 1, 5, 10, 15, 20°.

3. Results

The results of numerical analysis carried out on two load steps and on 4 femur models with different mechanical properties for femur – expandable intramedullary nail system are presented in Tables 1 and 2 and on Figs. 5 to 19.

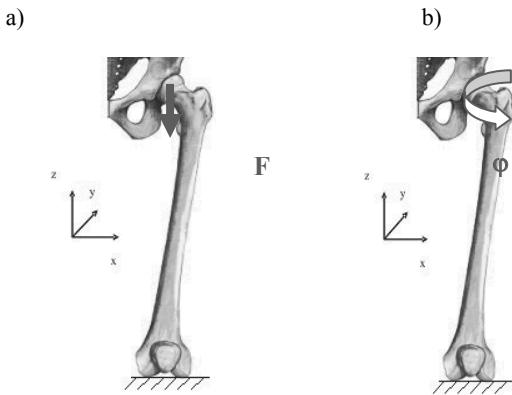


Fig. 4. Loading scheme of model: a) load step 1, b) load step 2

3.1. FEM analysis of the femur - intramedullary nail system - load step 1

Figures 5 to 11 present example distribution of displacements, deformations and reduced stresses in the femur - expandable intramedullary nail system determined for maximum load compressed with force 1000N (bone model 4 with mechanical properties corresponding with a femur of a patient at the age above 70 or with osteoporosis).

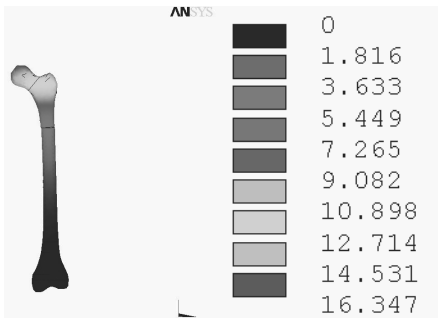


Fig. 5. Displacement vector sum distribution in femur - intramedullary nail system (compression force 1000N), mm - load step 1 bone model 4

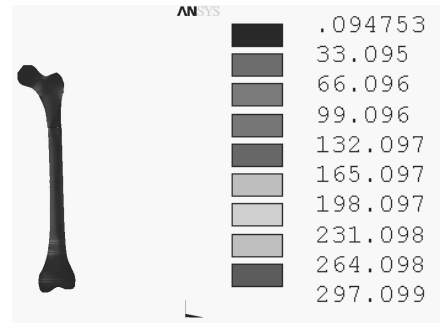


Fig. 6. Stress distribution in femur (compression force 1000N), MPa - load step 1, bone model 4

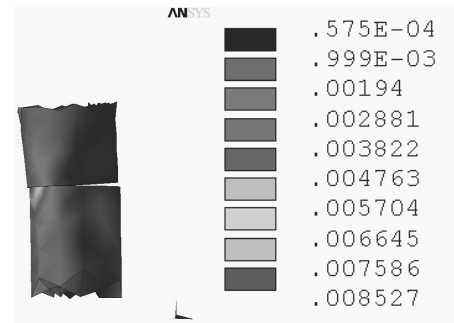


Fig. 7. Strain distribution in fracture gap x100% (compression force 1000N), % - load step 1, bone model 4

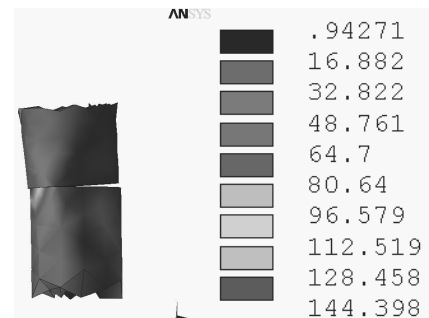


Fig. 8. Stress distribution in fracture gap (compression force 1000N), MPa - load step 1, bone model 4

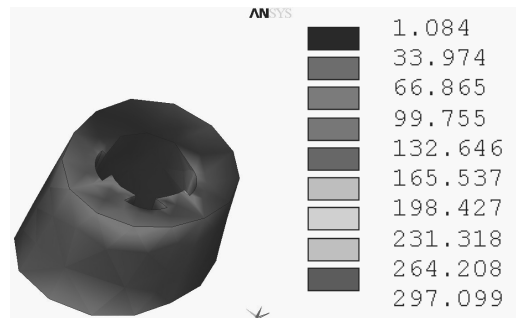


Fig. 9. Stress distribution in a place where expandable part of intramedullary nail is attached (compression force 1000N), MPa - load step 1, bone model 4

Table 1
The results of numerical analysis of the femur – expandable intramedullary nail system – load step 1

Intramedullary nail - femur system												
Force F, N	E=16000 MPa			E=22000 MPa			E=18600 MPa			E=17400 MPa		
	Displacement D, mm	Total Mechanical Strain ϵ , %	von Misses Stress σ , MPa	Displacement D, mm	Total Mechanical Strain ϵ , %	von Misses Stress σ , MPa	Displacement D, mm	Total Mechanical Strain ϵ , %	von Misses Stress σ , MPa	Displacement D, mm	Total Mechanical Strain ϵ , %	von Misses Stress σ , MPa
250	4.371	1	983	3.91	1	957	4.141	1	971	4.239	1	976
500	7.958	2.3	2134	6.83	2.2	2056	7.394	2.3	2097	7.636	2.3	2113
750	12.165	3.9	3540	10.179	3.7	3360	11.153	3.8	3447	11.6	3.8	3492
1000	17.231	5.9	5305	14.17	5.5	4980	15.687	5.7	5149	16.347	5.8	5216

Femur												
Force F, N	E=16000 MPa			E=22000 MPa			E=18600 MPa			E=17400 MPa		
	Displacement D, mm	Total Mechanical Strain ϵ , %	von Misses Stress σ , MPa	Displacement D, mm	Total Mechanical Strain ϵ , %	von Misses Stress σ , MPa	Displacement D, mm	Total Mechanical Strain ϵ , %	von Misses Stress σ , MPa	Displacement D, mm	Total Mechanical Strain ϵ , %	von Misses Stress σ , MPa
250	4.371	0.4	70	3.91	0.3	76	4.141	0.3	73	4.239	0.4	72
500	7.958	0.8	136	6.83	0.6	143	7.394	0.7	139	7.636	0.7	138
750	12.165	1.3	210	10.179	0.9	217	11.153	1.1	213	11.6	1.2	212
1000	17.231	1.8	295	14.17	1.3	302	15.687	1.6	298	16.347	1.7	297

Intramedullary nail												
Force F, N	E=16000 MPa			E=22000 MPa			E=18600 MPa			E=17400 MPa		
	Displacement D, mm	Total Mechanical Strain ϵ , %	von Misses Stress σ , MPa	Displacement D, mm	Total Mechanical Strain ϵ , %	von Misses Stress σ , MPa	Displacement D, mm	Total Mechanical Strain ϵ , %	von Misses Stress σ , MPa	Displacement D, mm	Total Mechanical Strain ϵ , %	von Misses Stress σ , MPa
250	3.466	1	983	3.097	1	957	3.281	1	971	3.36	1	976
500	6.224	2.3	2134	5.322	2.2	2056	5.772	2.3	2097	5.966	2.3	2113
750	9.449	3.9	3540	7.864	3.7	3360	8.64	3.8	3447	8.997	3.8	3492
1000	13.317	5.9	5305	10.879	5.5	4980	12.085	5.7	5149	12.611	5.8	5216



Fig. 10. Stress distribution in a place of a bolt (compression force 1000N), MPa- load step 1, bone model 4

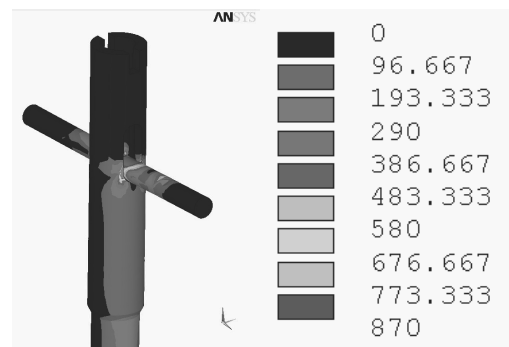


Fig. 11. Stress distribution in a place of a contact between a bolt and intramedullary nail (compression force 1000N), MPa- load step 1, bone model 4

Table 2.
The results of numerical analysis of the femur – expandable intramedullary nail system – load step 2

Intramedullary nail - femur system												
Angular displacement φ , °	E=16000 MPa			E=22000 MPa			E=18600 MPa			E=17400 MPa		
	Displacement D, mm	Total Mechanical Strain ϵ , %	von Misses Stress σ , MPa	Displacement D, mm	Total Mechanical Strain ϵ , %	von Misses Stress σ , MPa	Displacement D, mm	Total Mechanical Strain ϵ , %	von Misses Stress σ , MPa	Displacement D, mm	Total Mechanical Strain ϵ , %	von Misses Stress σ , MPa
1	1.345	0.09	87	1.343	0.09	89	1.344	0.09	88	1.344	0.09	88
5	6.724	0.4	438	6.716	0.4	449	6.48	0.4	444	6.721	0.4	442
10	13.447	0.9	877	13.432	0.9	899	13.439	0.9	888	13.44	0.9	884
15	20.171	1.4	1317	20.148	1.4	1349	20.159	1.4	1333	20.14	1.4	1326
20	26.855	1.8	1756	26.836	1.9	1799	26.878	1.8	1777	26.885	1.8	1768
Femur												
Angular displacement φ , °	E=16000 MPa			E=22000 MPa			E=18600 MPa			E=17400 MPa		
	Displacement D, mm	Total Mechanical Strain ϵ , %	von Misses Stress σ , MPa	Displacement D, mm	Total Mechanical Strain ϵ , %	von Misses Stress σ , MPa	Displacement D, mm	Total Mechanical Strain ϵ , %	von Misses Stress σ , MPa	Displacement D, mm	Total Mechanical Strain ϵ , %	von Misses Stress σ , MPa
1	1.345	0.09	14	1.343	0.07	16	1.344	0.08	15	1.344	0.08	14
5	6.724	0.4	70	6.716	0.3	82	6.48	0.4	75	6.721	0.4	73
10	13.447	0.9	140	13.432	0.7	165	13.439	0.8	150	13.44	0.8	146
15	20.171	1.4	210	20.148	1.1	248	20.159	1.2	226	20.14	1.3	219
20	26.855	1.8	280	26.836	1.5	330	26.878	1.7	301	26.885	1.7	292
Intramedullary nail												
Angular displacement φ , °	E=16000 MPa			E=22000 MPa			E=18600 MPa			E=17400 MPa		
	Displacement D, mm	Total Mechanical Strain ϵ , %	von Misses Stress σ , MPa	Displacement D, mm	Total Mechanical Strain ϵ , %	von Misses Stress σ , MPa	Displacement D, mm	Total Mechanical Strain ϵ , %	von Misses Stress σ , MPa	Displacement D, mm	Total Mechanical Strain ϵ , %	von Misses Stress σ , MPa
1	0.946	0.09	87	0.944	0.09	89	0.945	0.09	88	0.945	0.09	88
5	4.732	0.4	438	4.721	0.4	449	4.726	0.4	444	4.729	0.4	442
10	9.464	0.9	877	9.411	0.9	899	9.452	0.9	888	9.457	0.9	884
15	14.196	1.3	1317	14.162	1.4	1349	14.179	1.4	1333	14.186	1.4	1326
20	18.928	1.8	1756	18.883	1.9	1799	18.905	1.8	1777	18.915	1.8	1768

3.2. FEM analysis of the femur - intramedullary nail - load step 2

Figures from 12 to 19 show example distribution of displacements, deformations and reduced stresses in the femur – expandable intramedullary nail system determined for maximum angular displacement 20° in bone model 4 with mechanical properties corresponding with a femur of a patient at the age above 70 or with osteoporosis.

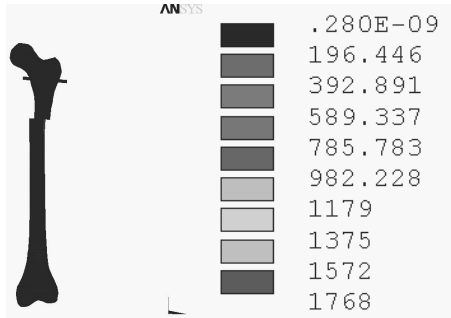


Fig. 14. Stress distribution in femur - intramedullary nail system (torsional angel 20°), MPa - load step 2 bone model 4

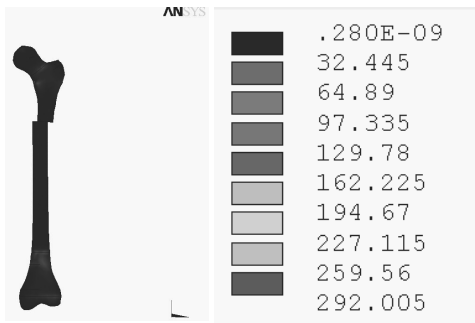


Fig. 15. Stress distribution in femur (torsional angel 20°), MPa- load step 2 bone model 4

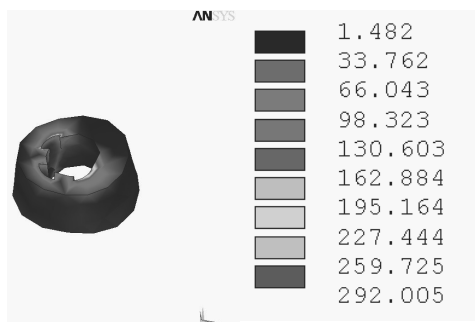


Fig. 16. Stress distribution in a place where expandable part of intramedullary nail is attached (torsional angel 20°), MPa - load step 2 bone model 4

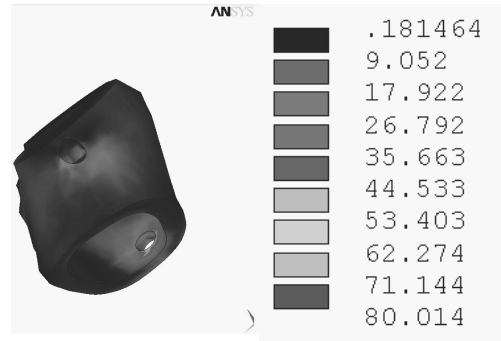


Fig. 17. Stress distribution in a place of a bolt (compression force 1000N) (torsional angel 20°), MPa - load step 2 bone model 4



Fig. 18. Stress distribution in a place of a contact between a bolt and intramedullary nail (torsional angel 20°), MPa - load step 2 bone model 4

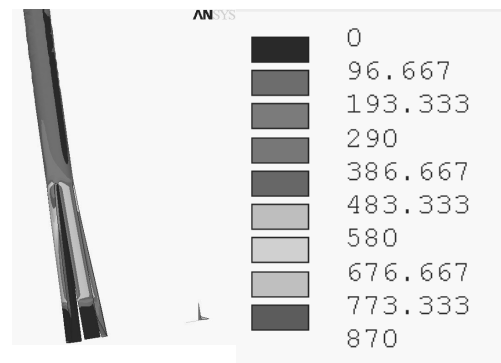


Fig. 19. Stress distribution in a place of a contact between the expandable part of intramedullary nail and femur (torsional angel 20°), MPa - load step 2 bone model 4

Obtained results of numerical calculations of the two load steps and four models with different mechanical properties of femur enabled preparing graphs of relations between obtained values of reduced deformations and reduced stresses depending on loading force in a case (load step 1) – Fig. 20 and 21 and

deformations and reduced stresses depending on the assumed torsional angle (load step 2) Fig. 22 and 23.

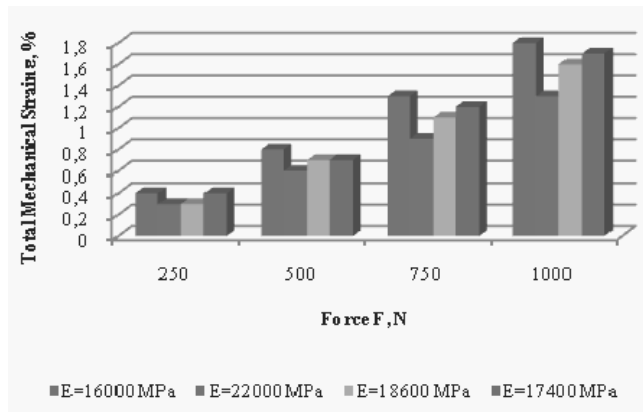


Fig. 20. Comparison of max total mechanical strain for all analyzed models, % - load step 1

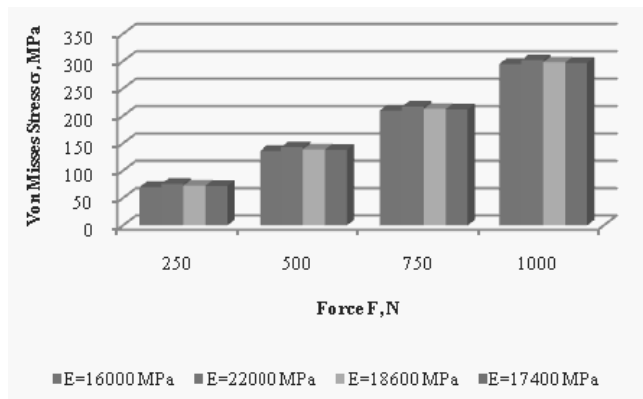


Fig. 21. Comparison of max von Mises Stress for all analyzed models, MPa - load step 1

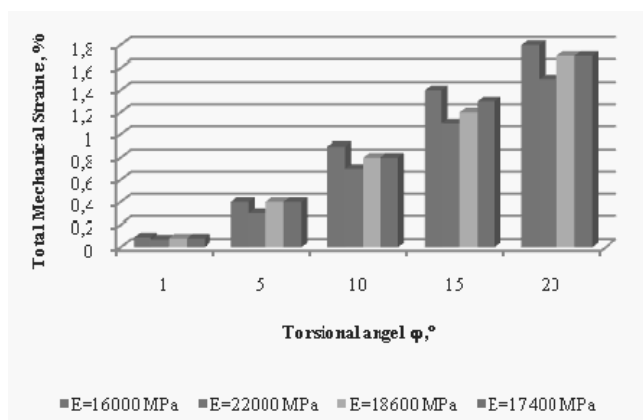


Fig. 22. Comparison of max total mechanical strain for all analyzed models, % - load step 2

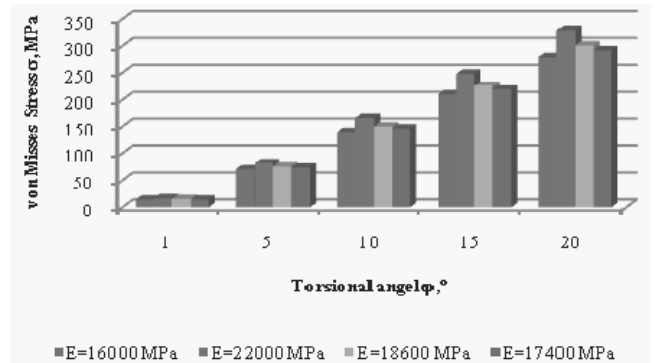


Fig. 23. Comparison of max von Mises Stress for all analyzed models, MPa - load step 2

On the basis of the conducted analysis of obtained results for the first load step, it can be stated that regardless of the values of Young's model for separate models with different mechanical properties of the bone, obtained values of reduced strains were similar. These values were minimal for the load 250N and amounted to 295 do 298 MPa. That means that for this load stains in some points exceeded values acceptable for proper bone function, which is 225 MPa. Exceeding these values may lead to damages or preventing damaged bone tissue from regenerating. Obtained in this part of paper results of reduced deformations were different depending on mechanical properties of femur. Maximum values of deformations were registered for model 1 and 4 with the loading force 100N and amounted appropriately to 1.8 and 1.7%.

The analysis of the results of the torsion of the femur – expandable intramedullary nail system showed that at the moment of the torsion of the femur head with the angle 15° maximum reduced strain for model 2, and with the angle 20° for all models occurs the extension of the acceptable values of stresses in a bone in a place of the contact between the expandable part of the nail and bone tissue. It proves that there is a possibility of the nail becoming loose and damaging the creating fibrocartilage callus. Similarly to compression analysis, maximum values of deformations were registered in models 1 and 4 and amounted appropriately 1.8 and 1.7%.

4. Conclusions

In order to conduct numerical analysis using Finite Element Method it is necessary to assume mechanical properties of materials used in the analysis (Young modulus, Poisson's ratio). In the paper mechanical properties of titanium alloy Ti-6Al-4V and bones of a human at different ages with Young modulus values based on literature were used. Analyzing obtained results of calculations it is necessary to consider also a bone density changing with age, which is especially important in case of osteoporosis and in addition, it influences the bone resistance to load.

The numerical analysis of the femur - expandable intramedullary nail system carried on four models with different mechanical properties of femur and 2 load steps (compression and torsion) showed, that the age of a patient and the state of femur

have influence on obtained values of displacements, deformations and reduced stresses. In case of fractures in the treatment of which intramedullary methods are used, the selection of an appropriate implant should be dependant above all on the age and state of patient's general conditions of bones in which particularly important is bone density.

The analysis of obtained results showed that with the appropriate load type and mechanical properties of femur there is a risk of damaging the bone in a place where fragments join or in a place where the expandable part of the nail is attached to the femur in its lower part. The lower the bone density caused by osteoporosis is, the bigger the risk of damages will be.

The possibility that the expandable intramedullary nail will become loose in the lower part of femur during torsion creates problem, which must be solved by appropriate design this part of an implant before beginning clinical research using the analyzed implant.

References

- [1] M. Nałęcz, Biocybernetics and biomedical engineering. 2000. Vol 5: Biomechanics and rehabilitation engineering PAN Academic Publishing House EXIT, Warszawa 2004, 1-42, 291-304 (in Polish).
- [2] R. Będziński, Engineering biomechanics. Selected issues, Publishing House of Wrocław Technical University, Wrocław, 1997, 13-45 (in Polish).
- [3] Master thesis: M. Krykant (2006).
- [4] A. Kajzer, W. Kajzer, J. Marciniak, Numerical and experimental analysis of the new, expansion intramedullary nails. *Engineering of Biomaterials* 89-91/XII (2009)114-118.
- [5] A. Ziębowicz, A. Kajzer, W. Kajzer, J. Marciniak, Biomechanical analysis of metatarsal bone "I"- compression screws system. *Engineering of Biomaterials* 89-91/XII, (2009) 246-249.
- [6] W. Kajzer, A. Kajzer, J. Marciniak, FEM analysis of compression screws used for small bone treatment. *Journal of Achievements in Materials and Manufacturing Engineering* 33/2 (2009) 189-196.
- [7] J. Marciniak, W. Chrzanowski, A. Krauze, Intramedullary nailing in osteosynthesis, Printing House of the Silesian University of Technology, Gliwice, 2006.
- [8] W. Walke, Z. Paszenda, J. Filipiak, Experimental and numerical biomechanical analysis of vascular stent, Proceedings of the 13th International Scientific Conference on "Achievements in Materials and Mechanical Engineering AMME'2005", Gliwice-Wisła, 699-702.
- [9] W. Walke, Z. Paszenda, J. Filipiak, Experimental and numerical biomechanical analysis of vascular stent, *Journal of Materials Processing Technology* 164-165 (2005) 1263-1268.
- [10] F. Jaroszyk, Biophysics - students textbook Medical Publishing House PZWL, Warszawa, 2001, 413-429.
- [11] A. Krauze, J. Marciniak, Numerical method in biomechanical analysis of intramedullary osteosynthesis in children. Proceedings of the 11th International Scientific Conference CAM3S'2005 "Contemporary Achievements in Mechanics, Manufacturing and Materials Science". Gliwice-Zakopane 2005, 528-533.
- [12] M. Kaczmarek, J. Marciniak, Issues of plate stabilizers for osteosynthesis Proceedings of the 3rd Scientific Conference "Materials, Mechanical and Manufacturing Engineering", Gliwice-Wisła 2005, 325-334.
- [13] M. Kaczmarek, J. Marciniak, J. Szewczenko, A. Ziębowicz, Plate stabilizers in elastic osteosynthesis. Proceedings of the 11th International Scientific Conference CAM3S'2005 "Contemporary Achievements in Mechanics, Manufacturing and Materials Science", Gliwice-Zakopane, 2005, 436-443.
- [14] A. Krauze, J. Marciniak, Numerical method in biomechanical analysis of intramedullary osteosynthesis in children. *Journal of Achievements in Materials and Manufacturing Engineering* 15 (2006) 120-126.
- [15] J. Okrajni, M. Plaza, S. Ziemia, Validation of computer models of an artificial hip joint. *Archives of Materials Science and Engineering*, 28/5 (2007) 305-308.
- [16] W. Chrzanowski, J. Marciniak, Biomechanical analysis of the femoral bone-interlocking intramedullary nail system. Proceedings of the 18th European Conference on Biomaterials, 2003, Germany, 154.
- [17] J. Marciniak, W. Chrzanowski, M. Kaczmarek, Biomechanical analysis of femur-intramedullar nail system with the use of finite element method, *Biomaterials Engineering* 30-33 (2003) 53-55.
- [18] W. Chrzanowski, J. Marciniak, Biomechanical and biomaterial conditions in intramedullar osteosynthesis. Proceedings of the 3rd Scientific Conference "Materials, Mechanical and Manufacturing Engineering", Gliwice-Wisła, 2005, 319-324.